Poly(L-glutamic acid)-co-poly(ethylene glycol) block copolymers for protein conjugation

Poly(L-glutamic acid)-co-poly(ethylene glycol) block copolymers for protein conjugation

Katia Maso[a,§], Antonella Grigoletto[a,§], Lucia Raccagni[a], Marino Bellini[a], Ilaria Marigo[b], Vincenzo Ingangi[b], Akira Suzuki[c], Midori Hirai[c], Masaki Kamiya[c], Hiroki Yoshioka[c], Gianfranco Pasut[*a]

a. Department of Pharmaceutical and Pharmacological Sciences, University of Padua, via F. Marzolo 5, 35131 Padua, Italy
b. Veneto Institute of Oncology IOV - IRCCS, Padua, Italy
c. NOF CORPORATION, DDS Research Laboratory, 3-3 Chidori-Cho, Kawasaki-Ku, Kawasaki, Kanagawa, 210-0865, Japan

[§]These authors contributed equally

Address correspondence to:
gianfranco.pasut@unipd.it
Tel. 0039 049 8275694
Fax 0039 049 8275366
Address: Department of Pharmaceutical and Pharmacological Sciences, University of Padua, via F. Marzolo 5, 35131 Padua, Italy

ABSTRACT

Poly(L-glutamic acid)-co-poly(ethylene glycol) block copolymers (PLE-PEG) are here investigated as polymers for conjugation to therapeutic proteins such as granulocyte colony stimulating factor (G-CSF) and human growth hormone (hGH). PLE-PEG block copolymers are able to stabilize and protect proteins from degradation and to prolong their residence time in the blood stream, features that are made possible thanks to PEG's intrinsic properties and the simultaneous presence of the biodegradable anionic PLE moiety. When PLE-PEG copolymers are selectively tethered to the N-terminus of G-CSF and hGH, they yield homogeneous monoconjugates that preserve the protein's secondary structure. During the current study the pharmacokinetics of PLE_{10}-PEG_{20k}-G-CSF and PLE_{20}-PEG_{20k}-G-CSF derivatives and their ability to induce granulopoiesis were, respectively, assessed in Sprague-Dawley rats and in C57BL6 mice. Our results show that the bioavailability and bioactivity of the derivatives are comparable to or better than those of PEG_{20k}-Nter-G-CSF (commercially known as Pegfilgrastim). The therapeutic effects of PLE_{10}-PEG_{20k}-hGH and PLE_{20}-PEG_{20k}-hGH derivatives tested in hypophysectomized rats demonstrate that the presence of a negatively charged PLE block enhances the biological properties of the conjugates additionally with respect to PEG_{20k}-Nter-hGH.

Keywords: protein delivery, polymer conjugation, PEGylation, human growth hormone, G-CSF

INTRODUCTION

As proteins present several advantages over low molecular weight drugs, a number of research groups have been striving to develop therapeutic proteins over the last 30-40 years. Proteins, in fact, are usually very specific and normally do not interfere with regular biological processes apart from the target one. They present nevertheless important deficiencies depending on some of their intrinsic features such as sensitivity to proteolytic enzymes, physical and chemical instabilities, immunogenicity and rapid body clearance even when they exceed the renal filtration threshold. The sum and complexity of these problems has limited the exploitation of at least some proteins as drugs simply because they are inconvenient or cannot meet the patient compliance owing the need of frequently dosage schedules of parenteral injections. Researchers are continuing to investigate more appealing solutions for protein delivery.

Of the various alternatives that have already been examined, polymer conjugation to proteins has distinguished itself as an efficacious strategy, and poly(ethylene glycol) (PEG) has become the gold standard among several polymers. PEGylation conveys stealth properties to proteins and increases their hydrodynamic volume, thus prolonging their blood half-life and partially reducing their instability and immunogenicity [1,2].

Although antibodies against PEG can be formed when it is administered with immune adjuvants, PEG is presently considered a safe non-immunogenic polymer, and several PEGylated proteins are now clinically available [3,4]. Anti-PEG antibodies have been detected in patients treated with PEG-uricase and PEG-asparaginase [5–7] as well as in naïve patients, presumably in connection to the use of PEG and PEG derivatives in body care products such as soaps, creams, shampoos, etc. Studies examining the role of anti-

PEG antibodies are currently underway. It has been found that the majority of anti-PEG antibodies have a low affinity versus PEG, and their presence is not connected with any pathological state [8,9].

PEG is non-biodegradable under normal *in vivo* conditions. Some PEGylated proteins can lead to the formation of vacuoles in certain specific cells, mainly macrophages, especially when conjugates are used at elevated doses and the polymer has a high molecular weight (≥40 kDa). While lysosomal enzymes can efficiently process proteins, polymers may long persist in lysosomes resulting in lysosomal distension and vacuolation [10,11]. The elimination of PEGs from vacuoles requires time and cannot be attributed to any specific process as it primarily depends on cell turnover. Until now, none of the conjugates in clinical use have shown toxic consequences linked to the vacuoles nor have they been connected with pathological states. Moreover, as partial or total reversibility of the vacuoles has been demonstrated when the therapeutic conjugate is suspended, it does not seem to constitute a relevant threat to PEG applications. Nonetheless, many researchers are investigating alternative polymers (some biodegradable and others not) such as polyglutamic acid (a negatively charged and biodegradable polymer [12]), polysarcosine (a biodegradable polypeptoid based on the amino acid sarcosine, i.e. N-methyl glycine, [13–15]), hyaluronic acid (a biodegradable polysaccharide composed of glucuronic acid and N-acetyl glucosamine [16–18]), polysialic acid (a biodegradable polysaccharide of N-acetylneuraminic acid [19–21]), poly-2-ethyl-2-oxazoline (a non-biodegradable polymer, [22–25]), etc.

In the effort to exploit PEG's ability to stabilize and protect proteins, the current study set out to investigate the use of poly(L-glutamic acid)-co-poly(ethylene glycol) block-co-polymers (PLE-PEG) as conjugating polymers for protein delivery in order to further improve the pharmacokinetic properties of the conjugate thanks to the biodegradable PLE moiety [26–29]. Anionic compounds such as PLE have been associated with slower renal ultrafiltration with respect to their positive or neutral counterparts, owing to the charge selectivity of the glomerular capillary wall of the kidneys. The glomerular capillary wall consists of three distinct, closely interacting layers: the fenestrated endothelium, comprising the glycocalyx; the podocytes, with their interdigitated foot processes and slit diaphragms; and the intervening glomerular basement membrane [30]. Several studies have confirmed that the glomerular capillary wall barrier is negatively charged and is able to discriminate between macromolecules depending on their size and net charge [31]. This effect holds true not only for polymers, such as dextran [32] and Ficoll [33], but also for proteins such as peroxidase [34], lactate dehydrogenase [35], etc. Block PLE-PEG co-polymers might take advantages of both PEG and PLE features as they have long lasting pharmacokinetic properties and a biodegradable PLE moiety [36] for overcoming the obstacle of cellular vacuolation linked to large PEGs.

Roncador *et al.* recently described the conjugation of the PLE-PEG co-polymer to alanine:glyoxylate aminotransferase (AGT), which was carried out by forming reversible disulphide bridges between the side chains of PLE, previously modified pyridyl dithiol, and the cysteine residues of the enzyme [37]. Consequently, in that specific case the polymer is link through the PLE linker and the PEG remained well exposed and, although the random approach of coupling, the polymer conjugation neither altered the protein's structure nor affected its enzymatic activity. In addition, the conjugate was found to be hemocompatible and stable in plasma.

Here we describe how PLE-PEG copolymers, composed of varying lengths of PLE and PEG blocks, can be site selectively conjugated by the PEG block to two model proteins, G-CSF and hGH, via chemical reductive amination at the proteins' N-terminus [38] or via transglutaminase mediated enzymatic conjugation to Gln residues [39–41]. In this study, the PEG remains covered by the PLE block and offered the possibility of a single site of conjugation on the protein surface. G-CSF and hGH were selected because beyond their pharmaceutical interest, they have been widely investigated in polymer conjugation, offering an opportunity of comparison, and also there are suitable animal models in which it is possible to test the pharmacodynamic profiles of the conjugates. In particular, G-CSF, which is an 18.8 kDa hematopoietic cytokine that regulates the proliferation and differentiation of neutrophilic granulocytes, is now used to overcome congenital and acquired neutropenia by improving the granulocyte count in neutropenic patients. The FDA approved recombinant human G-CSF in 1991 for the treatment of chemotherapy-induced neutropenia (the drug's generic name is filgrastim; its brand name is Neupogen®). The next generation of G-CSF, Pegfilgrastim, was released in 2002 as Neulasta®. In this case, a PEG_{20kDa} was N-terminal specifically conjugated to G-CSF to prolong the protein's circulation and protect it against premature degradation. hGH, also known as somatotropin, is a 22 kDa peptide hormone secreted by the anterior pituitary gland. Its recombinant form was approved in 1985 for the treatment of a number of conditions such as short stature in children (caused by growth hormone deficiency, GHD), adult GHD, and some diseases not related to GDH, including Turner's syndrome. hGH is administered subcutaneously (SC) on a daily basis, a therapeutic regimen that may be disagreeable to some patients/care-givers leading to poor compliance and adversely affecting therapeutic outcomes. In order to reduce the number of doses, a variety of long-acting hGH formulations have been developed, among which PEGylated analogues PHA-794428 (branched PEG_{40kDa} attached to the N terminus), NNC126-0083 (linear 43 kDa PEG tethered to Gln141) and ARX201 (linear PEG_{30kDa} linked to amino acid 35 in which the native tyrosine was substituted with p-acetylphenyl). Unfortunately, all needed to be terminated during Phase II clinical trials. Only Jintrolong, a PEGylated hGH derivative developed by GeneScience Pharmaceuticals, was approved in China in 2014 and is currently undergoing further clinical trials.

In this study, the *in vivo* potency of the protein conjugates was evaluated in animal models, the pharmacokinetics of the G-CSF conjugates were investigated in rats, and their ability to enhance granulopoiesis was evaluated in mice. Finally, the bioactivity of the hGH conjugates was tested in hypophysectomized rats. In this study, a thoroughly study of the best PEG-PLE candidates, namely PLE_{10}-PEG_{20k} and PLE_{20}-PEG_{20k} (the number in the PLE block indicates the quantity of L-glutamic monomers while in the case of PEG it indicates the MW) for the selected proteins is reported. Other tested candidates were PLE_{10}-PEG_{5k}, PLE_{50}-PEG_{5k} and PLE_{100}-PEG_{5k}, which although resulting in acceptable conjugation yields showed decreased stability of G-CSF and not satisfactory in vivo half-life prolongation, especially for the bigger PLE blocks.

EXPERIMENTAL

Materials

Recombinant human-G-CSF was generously provided by Sandoz (Ljubljana, Slovenia) and rh-hGH was acquired from Shenandoah Biotechnology (Warwick, PA, USA). Poly(L-glutamic acid)-co-poly(ethylene glycol) (PLE-PEG) block copolymers and PEGs were supplied by the NOF Corporation (Tokyo, Japan). All the chemicals and solvents were purchased from Sigma-Aldrich (Milano, Italy). Microbial TGase (mTGase), of *Streptomyces mobaraensis* origin (ACTIVA M), was kindly provided by the Ajinomoto Co. (Tokyo, Japan). Human G-CSF ELISA Kit was purchased from Life Technologies (Waltham, MA, USA). Precast gels for SDS-PAGE 4-15% were obtained from Bio-Rad (Milan, Italy).

Analytical methods

UV-Vis Spectroscopy

Protein concentrations were determined spectrophotometrically using a Thermo Scientific Evolution 201 spectrophotometer (Waltham, MA, USA) or by means of Bicinchoninic acid assay (BCA), as has been described elsewhere [42]. The absorbance of the proteins and protein conjugates was evaluated at 280 nm ($A^{0.1\%}_{280}$ G-CSF = 0.88, $A^{0.1\%}_{280}$ hGH = 0.794 and $A^{0.1\%}_{280}$ TGase = 1.89 ml cm^{-1} mg^{-1}). The extinction coefficients at 280 nm for the conjugated proteins were considered unvaried with respect to those of the native proteins. The values of the absorption at 280 nm were generated by ProtParam (http://www.expasy.org/tools/protparam.html).

Sodium dodecyl sulphate–polyacrylamide gel electrophoresis (SDS-PAGE)

Electrophoresis was performed following the Laemmli method [43]; the gels were stained with Blue Coomassie for protein detection and with iodine for PEG detection. Electrophoretic runs were carried out using an Electrophoresis Power Supply 300 (Pharmacia, NJ, USA).

Circular dichroism (CD) analysis

Far-UV circular dichroism spectra measurements were taken with a Jasco J-810 spectropolarimeter equipped with a Peltier temperature control unit at 25°C. G-CSF, hGH, and their derivatives were prepared at a protein concentration of 0.1 mg/ml in 10 mM acetate, 5% sorbitol pH 4.6 and PBS pH 7.4 containing 0.05% Tween 80, respectively. The spectra measurements between 200 and 250 nm were collected by an average of 3 scans, and the data at each wavelength were averaged for 8 s. The sample cell path length was 1 mm. The CD data were converted to mean residue ellipticity, expressed in deg cm^2 $dmol^{-1}$ by applying the $\Theta = \Theta_{obs}$ (MRW)/10L[C] formula where Θ_{obs} is the observed ellipticity in degrees, MRW is the mean residue weight of the protein, [C] is protein concentration in mg/ml, and L is the optical path length in centimetres. Thermal denaturation studies were conducted by increasing the temperature from 25 to 90°C, at a rate of 2°C/min, and measuring the ellipticity at 222 nm for G-CSF and at 208 nm for hGH.

Mass spectrometry analysis

Mass spectra data were obtained using a REFLEX time-of-flight instrument (4800 Plus MALDI TOF/TOF, AB Sciex, Framingham, MA, USA) equipped with a SCOUT ion source, operating in the positive linear mode. A pulsed UV laser beam (nitrogen laser, λ 337 nm) generated ions that were accelerated to 25 kV. Matrix (a saturated solution of sinapinic acid in water/ACN (1:1, v/v) + 0.1% TFA (v/v) was mixed with an equal volume of sample solution and 1-2 µl were loaded on the plate.

Analytical SEC-HPLC

Analytical size exclusion chromatography (SEC) was performed using a Biosep SEC-S3000 column (4.6 × 300 mm; 5 µm) operating at a flow rate of 0.35 ml/min. Elution experiments were conducted with 20 mM, 130 mM sodium chloride and 20% ACN pH 7; the absorbance was measured at 226 nm.

N-terminal PEGylation of G-CSF and hGH

1) Synthesis of PEG_{20k}-G-CSF and PEG_{40k}-G-CSF

G-CSF was dissolved in 10 mM sodium acetate, 5% (v/v) sorbitol pH 4.6, and 3 equivalents of monomethoxy PEG-aldehyde 20 or 40 kDa were added. After stirring for an hour at 4°C, $NaCNBH_3$ was added (100 equivalents with respect to the protein); the final G-CSF concentration was 3 mg/ml. The mixture was left to react under stirring for 24 hours at 4°C; it was monitored by RP-HPLC with a Jupiter C18 column (250 × 4.6 mm, 300 Å, 5 µm; Phenomenex, USA), eluted with H_2O + 0.1% TFA (eluent A) and ACN + 0.1% TFA (eluent B) at 1.0 ml/min flow-rate (gradient B%: 0' 40%, 25' 70%, 27' 90%, 29' 40% B). The effluent was monitored by measuring the absorbance at 226 nm. Gly-Gly (100 equivalents with respect to the protein) was added to stop the reaction. After an hour, the reaction mixture was dialyzed against 10 mM sodium phosphate buffer pH 4.7. The solution was recovered after dialysis, and the PEG-G-CSF conjugates were purified by cation exchange chromatography using a TSKgel SP-5PW column (7.5 × 75 mm; 10 µm) operating at a flow-rate of 1.0 ml/min and registering the absorbance at 280 nm (buffer A: 10 mM sodium phosphate pH 4.7 and buffer B: 100 mM sodium phosphate, 100 mM sodium chloride pH 4.85; gradient B%: 0' 5%, 5' 5%, 65' 100%, 80' 100%, 85' 5%). The peak of the conjugates was collected, concentrated with Amicon Ultra Centrifugal filters (cut off 10 kDa; 5000 × g at 4°C), and dialyzed against 10 mM sodium acetate, 5% (v/v) sorbitol pH 4.6.

2) Synthesis of PLE_{10}-PEG_{20k}-G-CSF and PLE_{20}-PEG_{20k} -G-CSF

PLE_{10}-PEG_{20k}-aldehyde or PLE_{20}-PEG_{20k}-aldehyde was conjugated to G-CSF under the same conditions outlined above for monomethoxy PEG-aldehyde 20 and 40 kDa with the single exception being that the incubation temperature was 25°C instead of 4°C. Before they were purified by cation exchange chromatography, the solutions were dialysed against 10 mM sodium phosphate buffer pH 4.5. In this case, a TSKgel SP-STAT column (4.6 × 100 mm; 7µm) operating at a flow rate of 0.7 ml/min was used (buffer A: 10 mM sodium phosphate pH 4.5; buffer B: 100 mM sodium phosphate pH 5.75; gradient B%: 0' 10%, 10' 10%,

70’ 80%, 75’ 100%, 80’10%. Wavelength 280 nm). The peak of the conjugates was collected, concentrated and, finally, dialyzed against 10 mM sodium acetate, 5% (v/v) sorbitol pH 4.6.

3) Synthesis of PEG_{20k}-hGH, PEG_{40k}-hGH, PLE_{10}-PEG_{20k}-hGH and PLE_{20}-PEG_{20k}-hGH

hGH was dissolved in 100 mM sodium acetate pH 5.5, and 5 equivalents of polymer (mPEG-aldehyde 20 or 40 kDa, PLE_{10}-PEG_{20k}-aldehyde or PLE_{20}-PEG_{20k}-aldehyde) were added. The reaction was stirred at 4°C for one hour after which $NaCNBH_3$ was added (50 equivalents with respect to the protein). The mixture obtained was incubated for 24 hours under stirring at 25°C. The final protein concentration was 1 mg/ml. The reaction was monitored with a Jupiter C18 column (250 × 4.6 mm, 300 Å, 5 µm; Phenomenex, USA) eluted with H_2O + 0.1% TFA (eluent A) and ACN + 0.1% TFA (eluent B) at 1.0 ml/min flow-rate (gradient B%: 0’ 40%, 25’ 80%, 27’ 90%, 29’ 40% B). The effluent was monitored at 226 nm. Gly-Gly (100 equivalents with respect to the protein) was added to stop the reaction, and the solution was left to react under stirring for 1 hour at 25°C. The mixture was then dialyzed against 10 mM sodium acetate pH 4.7 and purified by cation exchange chromatography with a TSKgel SP-STAT 7 µm column (100 × 4.6 mm) at a flow rate of 0.7 ml/min (buffer A: 10 mM sodium acetate pH 4.7; buffer B: 10 mM sodium acetate, 500 mM sodium chloride pH 4.85; gradient B%: 0’ 5%, 10’ 5%, 75’ 60%, 75’ 100%, 80’5%; Wavelength 280 nm). The purified peak of the conjugates was concentrated and dialyzed against PBS pH 7.4 containing 0.05% Tween 80.

Enzymatic conjugation of PLE_{10}-PEG_{5k}-NH_2, PLE_{50}-PEG_{5k}-NH_2 and PLE_{100}-PEG_{5k}-NH_2 copolymers to Gln135 of G-CSF via mTGase

G-CSF was dissolved in 10 mM sodium phosphate, 5% (v/v) sorbitol pH 8 and the PLE-PEG-NH_2 copolymer (10 equivalents of PLE_{10}-PEG_{5k}-NH_2, 3 equivalents of PLE_{50}-PEG_{5k}-NH_2 or 3 equivalents of PLE_{100}-PEG_{5k}-NH_2) was added. mTGase at a ratio of 1/50 enzyme/substrate (E/S) was then added; the final G-CSF concentration was 2 mg/ml. The reactions, which were stirred for 4 hours at 25°C, were stopped by adding N-ethylmaleimide (NEM) at a molar ratio of 1:0.8 with respect to mTGase. The reactions were monitored by RP-HPLC, as described above for the N-terminal PEGylation. The solutions were purified by dialysis against 10 mM sodium phosphate buffer pH 4.5 and by cation exchange chromatography with TSKgel SP-STAT 7 µm column (buffer A: 10 mM sodium phosphate pH 4.5; buffer B: 100 mM sodium phosphate pH 5.75; gradient B% for PLE_{10}-PEG_{5k}-Gln-G-CSF: 0’10%, 10’10%, 70’80%, 75’80%, 80’100%; gradient B% for PLE_{50}-PEG_{5k}-Gln-G-CSF: 0’2%, 10’2%, 70’100%, 75’2%; gradient B% for PLE_{100}-PEG_{5k}-Gln-G-CSF: 0’2%, 10’2%, 75’100%, 80’2%; wavelength 280 nm; flow rate 0.7 ml/min). The purified products were concentrated and dialyzed against 10 mM sodium acetate, 5% (v/v) sorbitol pH 4.6.

Pharmacokinetic study of N-terminal PLE-PEG-G-CSF conjugates in rats

The pharmacokinetic profiles of the G-CSF and G-CSF conjugates (PEG_{40k}-Nter-G-CSF, PEG_{20k}-Nter-G-CSF, PLE_{10}-PEG_{20k}-Nter-G-CSF and PLE_{20}-PEG_{20k}-Nter-G-CSF) in female Sprague-Dawley rats weighing between 200 g and 270 g (n = 3 for G-CSF group; n = 4 per group for conjugates) were determined. The samples were

prepared in phosphate buffered saline (PBS) pH 7.4, and a dose of 100 μg/kg (G-CSF equiv.) was intravenously injected into the lateral tail vein of the rats which were anesthetized with 5% isoflurane gas mixed with O_2 in the enclosed cages. Blood samples were collected from the anesthetized rats using the tail incision method at predetermined time points and centrifuged at 1500 × g for 20 min. The G-CSF concentration in the serum was quantified using a Human G-CSF ELISA Kit (Life Technologies). The pharmacokinetic data were analyzed using 2.0 PkSolver software after a bi-compartmental model was fitted.

The *in vivo* activity of N-terminal PLE-PEG-G-CSF conjugates

The effect of PLE-PEG copolymers conjugation to G-CSF on immune cells counts was evaluated *in vivo* in C57BL/6 female mice of 8 weeks (18-20 g) purchased from Charles River Laboratories.

To assess the ability to induce myeloid accumulation the conjugates were injected subcutaneously as a single dose of 1 mg/kg of G-CSF equiv. (4 mice per group). G-CSF was also administrated at the same dose. Vehicle solution (PBS) was used as control. Blood samples were collected at days 3 and 5 and at day 7 the mice were sacrificed, and their spleens were harvested to be analysed.

Myeloid cell (monocytes and granulocytes) accumulation induced by not conjugated cytokine was evaluated by subcutaneously injecting G-CSF (3 mice per group) with a single dose of 2.5 or 5 mg/kg or as daily dose of 1 mg/kg of G-CSF. Vehicle solution (PBS) was used as control. The effect was evaluated at different time points in blood (24, 48, and 72 hours) or spleen (day 7).

Injected samples were prepared using sterile water and resulted negative to the LAL test (endotoxin levels < 5 EU/ml). The quantification of myeloid cells sub-populations in blood or spleen was performed by FACS analysis after staining with specific markers and defined on live cell gate as myeloid cells ($CD11b^+$); granulocytes ($CD11b^+Ly6C^{int}Ly6G^+$); monocytes ($CD11b^+Ly6C^{high}Ly6G^-$). Cytofluorimetric data were acquired with a BD LSR II flow cytometer and analyzed by FlowJo software.

The pharmacodynamics of the N-terminal PLE-PEG-hGH conjugates in the hypophysectomised rats

Twenty-four hypophysectomised male OVA rats were purchased from Charles River Laboratories (Lecco, Italy) and kept in the animal facility for two weeks until the experiment could be carried out. Weighing approximately 90 g when the study was initiated, the rodents were randomly divided into six groups (4 animals per group). The first group received a tail vein injection of 200 μl of vehicle solution (PBS). The second group received a daily tail vein injection of hGH for six days (the daily dose was 0.3 mg/kg). The other groups received a single tail vein injection on day 0 of 1.8 mg/kg (hGH equiv.) of hGH conjugates (PEG_{20k}-Nter-hGH, PEG_{40k}-Nter-hGH, PLE_{10}-PEG_{20k}-N-ter-hGH or PLE_{20}-PEG_{20k}-Nter-hGH). All the conjugates were solubilized in PBS. The animals were monitored and weighed at the same time every day until they were sacrificed on day 11. At the end of the experiments, the tibias were harvested and measured.

Ethics statement

The study protocol was approved by the Ethics Committee of the University of Padova and the Italian Ministry of Health. The animals were handled in compliance with Italian Legislative Decree 116/92 guidelines and in accordance with "The Guide for the Care and Use of Laboratory Animals" published by the National Research Council of the National Academies.

RESULTS AND DISCUSSION

PEG-aldehyde 20 kDa was tethered to N-terminal amino group of G-CSF to produce the commercially successful conjugate known as Neulasta. Site-specific coupling at the N-terminus exploits the lower *p*Ka of the α-amino group rather than the ε-amine lysines. At a slightly acidic pH, the ε-amino groups are protonated and are consequently not reactive toward low-reactive PEGylating agents such as PEG-aldehyde; the α-amino group instead preserves its reactivity thus yielding a homogeneous, well-characterized final product.

During the current study, the N-terminal PEGylation approach was applied to prepare G-CSF and hGH conjugates using PLE-PEG-aldehyde block copolymers. The work set out to examine the *in vivo* properties of the N-terminal derivatives of G-CSF and hGH that were produced with the PLE-PEG-aldehyde copolymers. The activity of these conjugates was compared to that of the unmodified protein and the N-terminal PEGylated derivatives with PEG 20 kDa and 40 kDa.

In addition to N-terminal conjugation, there is another well-known site specific PEGylation approach for proteins that exploits mTGase, an enzyme that catalyzes the acyl transfer between the γ-carboxamide group of a glutamine residue in the protein backbone and the aliphatic primary amine of a PEG-NH_2 [44,45]. As far as G-CSF is concerned, mTGase selectively conjugates the polymer to Gln135 out of 17 Gln residues [46]. Our study aimed to test the suitability of PLE-PEG-NH_2 copolymers as mTGase substrates using a block copolymer with a 5 kDa PEG moiety and higher glutamic acid levels in the PLE block, namely 10, 50 and 100 L-Glu units. The reaction mixtures underwent preliminary analyses by SDS-PAGE (Fig. S1) which established that all three block copolymers can accommodate in the catalytic site of mTGase after recognition of the Gln135 of G-CSF. The reactions' yields of conjugate formation were about 95% for PLE_{10}-PEG_{5k}-Gln135-G-CSF and around 60% for PLE_{50}-PEG_{5k}-Gln135-G-CSF and PLE_{100}-PEG_{5k}-Gln135-G-CSF conjugates. The G-CSF conjugates with PLE_{50}-PEG_{5k} or PLE_{100}-PEG_{5k} showed a decreased stability with respect of G-CSF, especially in the acidic buffer of G-CSF storage (pH 4.6), likely owing to the low solubility of the PLE block at this pH value. For the same reason of low solubility, such copolymers with a short PEG block are not suitable for N-terminus site specific conjugation because this reaction is carried out in acidic environment. When these PLE_x-PEG_{5k}-G-CSF were investigated in a preliminary pharmacokinetic study, they showed a not satisfactory pharmacokinetic profile, especially for those conjugates with PLE_{50} and PLE_{100} blocks (Fig. S2). Consequently, we developed and focused on PLE_{10}-PEG_{20k} or PLE_{20}-PEG_{20k} for a thoroughly study with two model proteins G-CSF and hGH. In order to directly compare G-CSF and hGH, we proceeded with N-terminal conjugation to evaluate the potential of PLE-PEG copolymers-protein conjugates *in vivo*.

As shown in the RP-HPLC profiles of the reaction solutions (Fig. 1, left panel), the yields of the conjugation of G-CSF via N-terminal coupling ranged between ~70 and ~76%. In the chromatograms, the peak at 22.2 min corresponded to unmodified G-CSF while the peaks eluting at lower retention times corresponded to the conjugates.

Following purification by cation exchange chromatography, the G-CSF conjugates were characterized by MALDI-TOF mass spectrometry, SDS-PAGE and circular dichroism. The MALDI-TOF spectra of the conjugates (Fig. S3) exhibited a molecular weight (MW) corresponding to the sum of the MWs of the protein (18.8 kDa, Fig. S4 A) and the polymer: PEG_{40k}-Nter-G-CSF (~61.7 kDa), PEG_{20k}-Nter-G-CSF (~40.3 kDa), PLE_{10}-PEG_{20k}-Nter-G-CSF (~40.6 kDa) and PLE_{20}-PEG_{20k}-Nter-G-CSF (~41 kDa). The theoretical MWs of PLE_{10}-PEG_{20k}-aldehyde and PLE_{20}-PEG_{20k}-aldehyde copolymers were calculated as 21510 Da and 23020 Da, respectively, considering the MW of the glutamic acid monomer in the sodium salt form (MW 151 Da).

The formation of G-CSF monoconjugates was confirmed by SDS-PAGE. In the gel (Fig. S5A) PEG_{40k}-Nter-G-CSF showed an apparent hydrodynamic volume of ~85 kDa; PEG_{20k}-Nter-G-CSF, PLE_{10}-PEG_{20k}-Nter-G-CSF and PLE_{20}-PEG_{20k}-Nter-G-CSF showed one of ~50 kDa. PEG's ability to coordinate on average five molecules of water for each ethylene glycol unit explains why PEGylated proteins appear larger in SDS-PAGE analysis. Overall, the MALDI-TOF and SDS-PAGE analysis demonstrated that G-CSF N-terminal monoconjugates were successfully obtained and purified from the native protein and the multi-PEGylated species.

G-CSF conjugates were also characterized by means of analytical size exclusion chromatography (Fig. S6); the results showed that the products were pure and that PEG 20 kDa, PLE_{10}-PEG_{20k} and PLE_{20}-PEG_{20k} derivatives presented a similar hydrodynamic volume (T_R 8.1 min).

The secondary structure of G-CSF and the conjugates was investigated by means of far-UV-CD in order to evaluate the effect of the polymers on the protein's surface. As expected, G-CSF has a predominantly α-helix structure [47] with two characteristic negative bands at ~212 and ~225 nm. As the CD spectrum of G-CSF was superimposable with those of the conjugates (Fig. 2A), it can be concluded that all the polymers tested, and therefore even the PLE-PEG block copolymers, did not modify the protein's conformation.

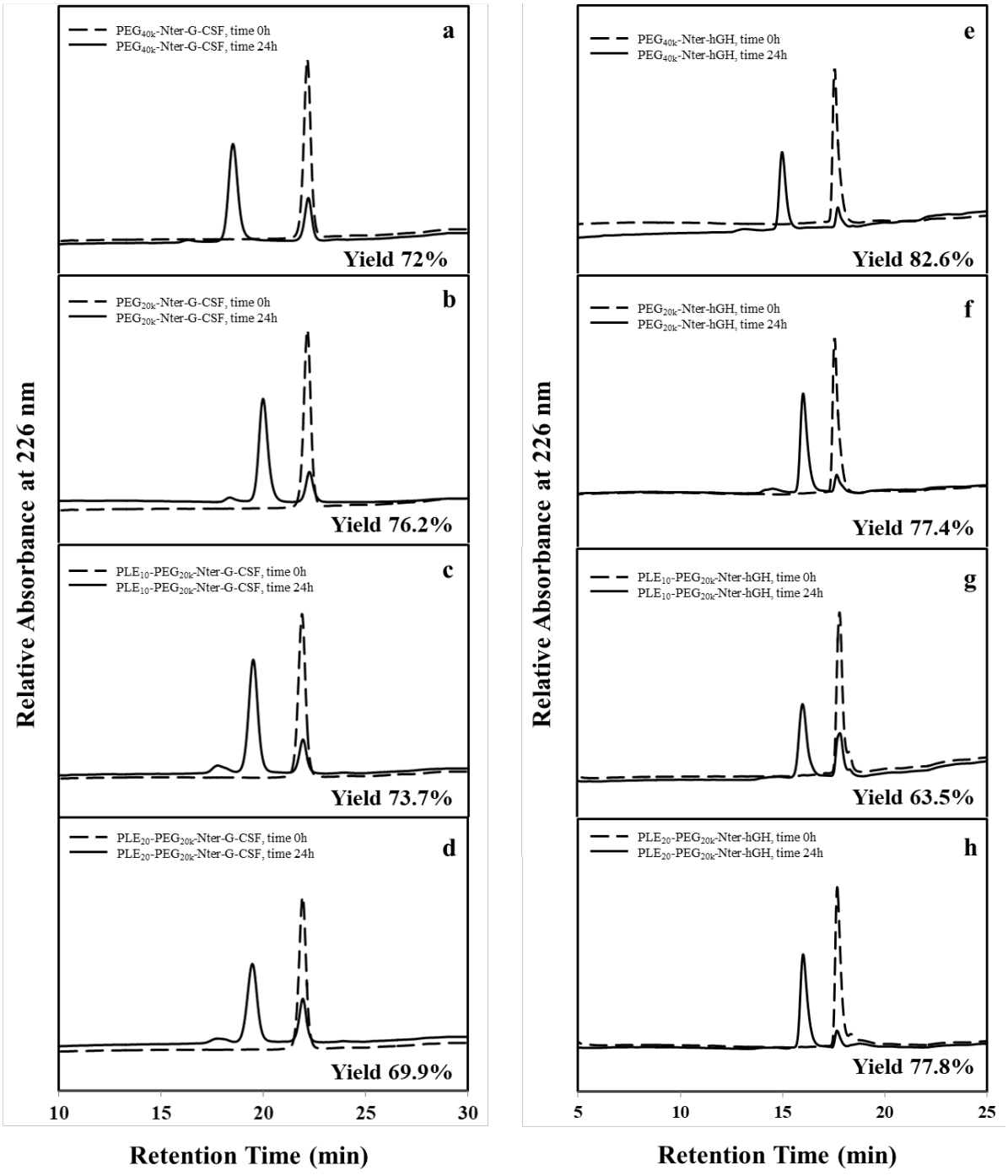

Figure 1. The continuous black lines represent the RP-HPLC profile at 226 nm of the reaction solutions used for the N-terminal PEGylation of G-CSF and hGH with PEG_{40k}-aldehyde (a, e) PEG_{20k}-aldehyde (b, f), PLE_{10}-PEG_{20k}-aldehyde (c, g) and PLE_{20}-PEG_{20k}-aldehyde (d, h). The dashed lines represent the RP-HPLC profile of the unmodified G-CSF (T_R 22.2 min, left panel) or of hGH (T_R 17.6 min, right panel). The reaction yields are listed at the lower right-hand corner of each panel.

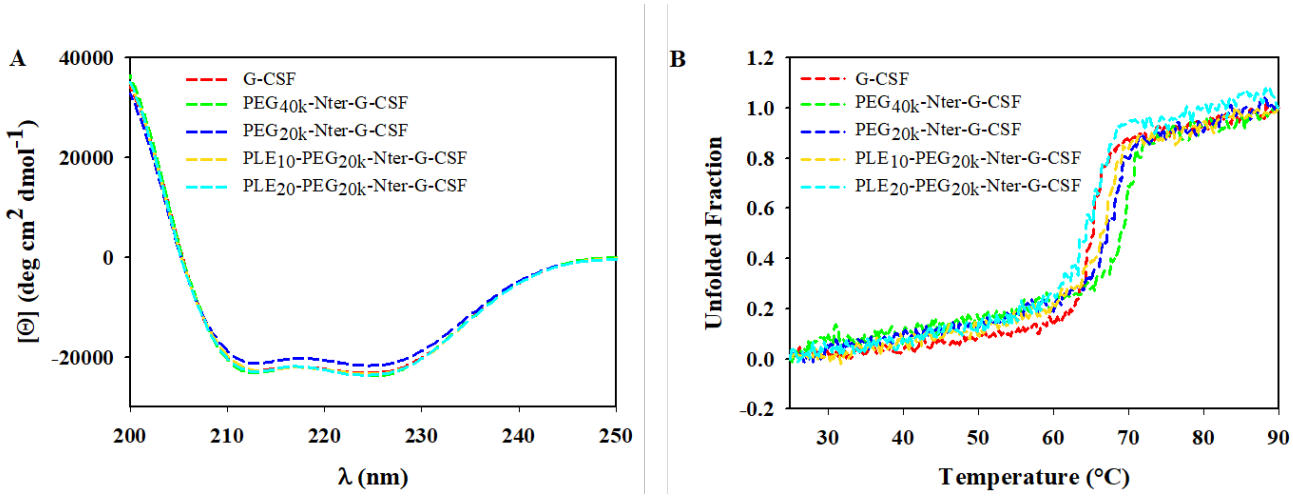

Figure 2. A) CD spectra and B) temperature dependence of the CD intensity at 222 nm of G-CSF, PEG_{40k}-Nter-G-CSF, PEG_{20k}-Nter-G-CSF, PLE_{10}-PEG_{20k}-Nter-G-CSF and PLE_{20}-PEG_{20k}-Nter-G-CSF. The samples were dissolved in 10 mM acetate, 5% (v/v) sorbitol pH 4.6 buffer at a protein concentration of 0.1 mg/ml.

Protein unfolding as a function of temperature was evaluated by recording the ellipticity at 222 nm of protein sample heated from 25 to 90°C. Melting temperatures (T_m), defined as the temperature at which 50% of the protein is unfolded, were calculated assuming that the protein was completely folded at 25°C and completely unfolded at 90°C. The melting profiles of G-CSF and its derivatives are outlined in Fig. 2B. The thermal stability of PEG_{40k}-Nter-G-CSF and PEG_{20k}-Nter-G-CSF increased by ~4°C and ~2°C, respectively, as compared to that of G-CSF, confirming that the presence of PEG protected against thermal stress. In the case of PLE-PEG block copolymers, the conjugation did not essentially change the unfolding process of G-CSF as the variation of the melting temperatures was not very significant (T_m of PLE_{10}-PEG_{20k}-Nter-G-CSF = +1.3°C and T_m of PLE_{20}-PEG_{20k}-Nter-G-CSF = -1°C with respect to that of G-CSF). The melting temperatures are listed in Table 1.

Table 1. The melting temperatures of G-CSF, PEG_{40k}-Nter-G-CSF, PEG_{20k}-Nter-G-CSF, PLE_{10}-PEG_{20k}-Nter-G-CSF and PLE_{20}-PEG_{20k}-Nter-G-CSF.

Compound	T_m [°C]
G-CSF	65.4 ± 0.1
PEG_{40k}-Nter-G-CSF	69.3 ± 0.2
PEG_{20k}-Nter-G-CSF	67.3 ± 0.14
PLE_{10}-PEG_{20k}-Nter-G-CSF	66.7 ± 0.16
PLE_{20}-PEG_{20k}-Nter-G-CSF	64.4 ± 0.55

We decided to use hGH as an additional protein model to investigate the effect of PLE-PEG copolymers on the protein's *in vivo* bioactivity. PEG_{40k}-Nter-hGH, PEG_{20k}-Nter-hGH, PLE_{10}-PEG_{20k}-Nter-hGH and PLE_{20}-PEG_{20k}-Nter-hGH were prepared using the same N-terminal PEGylation approach. The yields of the reactions, calculated from the area of the peaks in the RP-HPLC chromatograms, ranged between 63 and 83% as (Fig. 1, right panel). After purification, the hGH conjugates were characterized by MALDI-TOF mass spectrometry, SDS-PAGE and circular dichroism. The MALDI-TOF spectra of the conjugates (Fig. S7) exhibited a MW corresponding to the sum of the MWs of the protein (22 kDa, Fig. S4B) and the polymer: PEG_{40k}-Nter-hGH (~63.6 kDa), PEG_{20k}-Nter-hGH (~43.7 kDa), PLE_{10}-PEG_{20k}-Nter-hGH (~44.6 kDa) and PLE_{20}-PEG_{20k}-Nter-hGH (~44.6 kDa). In the SDS-PAGE analysis, the hGH monoconjugates appeared pure and with a higher MW with respect to the native protein, thus confirming that polymer conjugation had been successfully performed (Fig. S5B).

Far-UV CD spectra of the hGH and the conjugates were compared in order to evaluate the effect of the polymers on the protein's conformation. hGH has a predominantly α-helical structure with two characteristic bands at 222 and 208 nm. In this case as well, we found that PLE-PEG block copolymers led to conjugates, whose secondary structure of the native protein, was preserved. Superimpositions of the CD profiles are shown in Fig. 3A. Protein unfolding was evaluated by recording the ellipticity at 208 nm of the protein sample heated from 25 to 90°C. The melting profiles of hGH and its derivatives are shown in Fig. 3B. The thermal stability of the conjugates with respect to that of hGH remained essentially unchanged, as demonstrated by the only slight variations in the melting temperatures that were registered (Table 2).

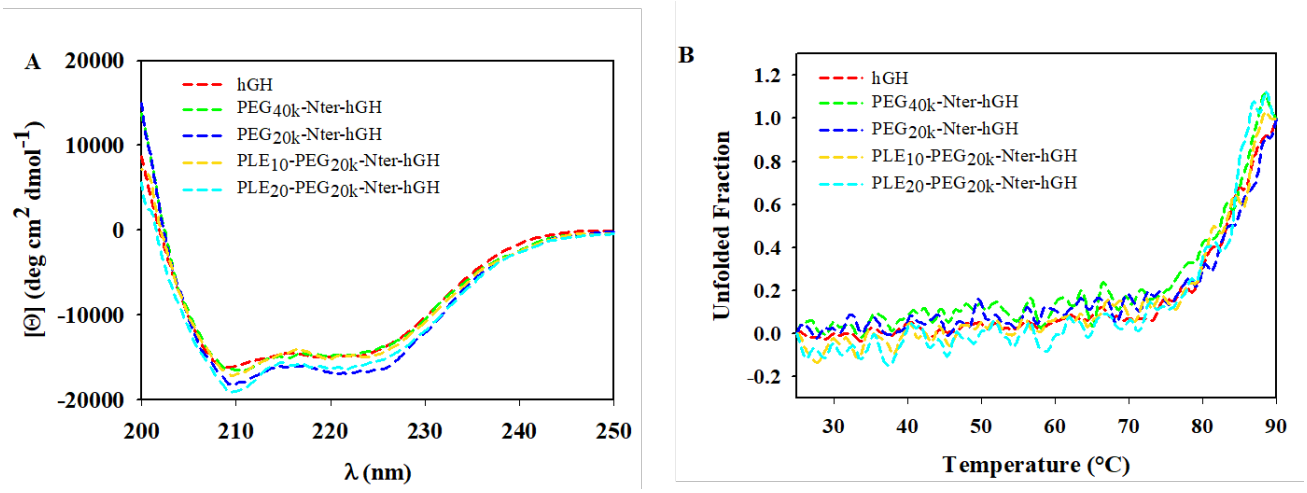

Figure 3. A) CD spectra and B) temperature dependence of the CD intensity at 208 nm of hGH, PEG_{40k}-Nter-hGH, PEG_{20k}-Nter-hGH, PLE_{10}-PEG_{20k}-Nter-hGH and PLE_{20}-PEG_{20k}-Nter-hGH. The samples were dissolved in PBS pH 7.4 containing 0.05% Tween 80 at a protein concentration of 0.1 mg/ml.

Table 2. The melting temperatures of hGH, PEG_{40k}-Nter-hGH, PEG_{20k}-Nter-hGH, PLE_{10}-PEG_{20k}-Nter-hGH and PLE_{20}-PEG_{20k}-Nter-hGH.

Compound	T_m [°C]
hGH	83.3 ± 0.26
PEG_{40k}-Nter-hGH	84.5 ± 0.22
PEG_{20k}-Nter-hGH	84.2 ± 0.32
PLE_{10}-PEG_{20k}-Nter-hGH	83.1 ± 0.2
PLE_{20}-PEG_{20k}-Nter-hGH	84.1 ± 0.14

Overall, the N-terminal G-CSF and hGH conjugation with PLE-PEGs with 10 or 20 glutamic acid units produced similar yields of polymer coupling; the monoconjugates were successfully purified and the native secondary structure of the protein was preserved.

Pharmacokinetic and pharmacodynamic experiments were carried out to evaluate how the presence of a negatively charged block copolymer affected the *in vivo* properties of the protein derivatives. The pharmacokinetics of G-CSF and its derivatives were studied in rats that had undergone an i.v injection in the lateral tail vein. As is illustrated in Fig. 4, immediately after the injection, high levels of native G-CSF were detected in the plasma, but the values fell rapidly and after a 7-hour period, the protein was essentially cleared from circulation. G-CSF conjugates could, instead, be detected in the plasma for 48 h.

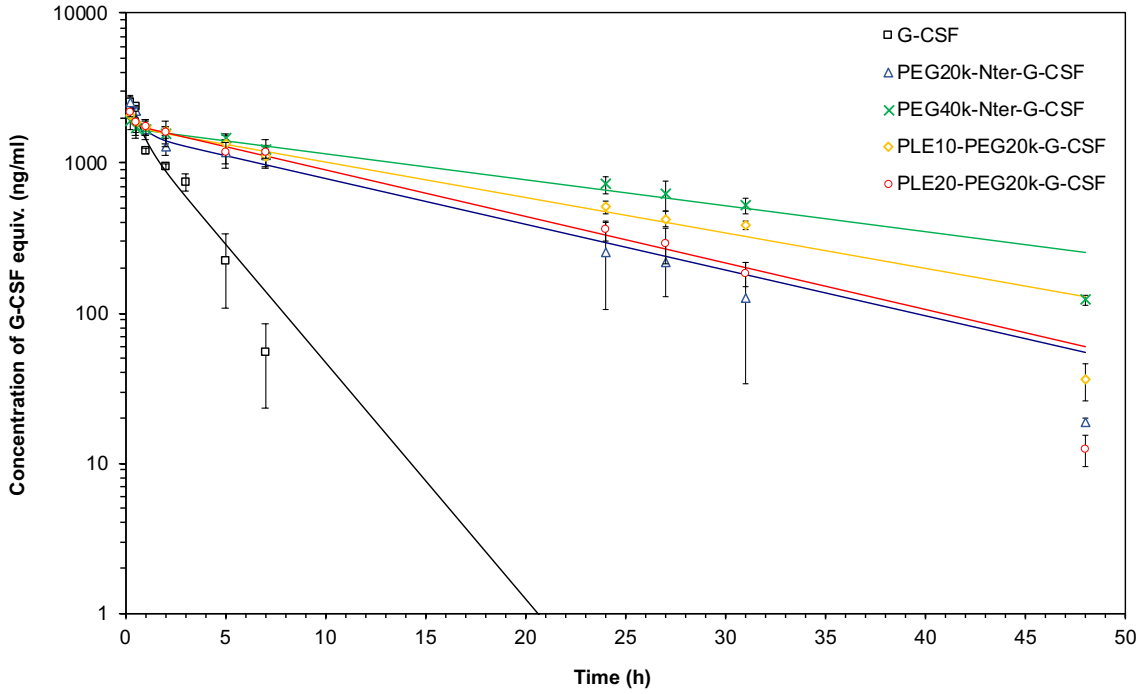

Figure 4. The pharmacokinetic profiles of G-CSF, PEG_{40k}-Nter-G-CSF, PEG_{20k}-Nter-G-CSF, PLE_{10}-PEG_{20k}-Nter-G-CSF and PLE_{20}-PEG_{20k}-Nter-G-CSF in Sprague Dawley rats (n = 3 for G-CSF group; n = 4 per group

for conjugates) after i.v. administration of 100 μg/kg G-CSF (protein equiv.). The data are presented as mean ± SD. * $p < 0.01$ vs. G-CSF (significance was calculated using ANOVA).

The proteins' principal pharmacokinetic parameters are outlined in Table 3. Conjugation to the multicarboxylic PLE-PEG block copolymers did not have a negative effect on the pharmacokinetics of the conjugates, and the residence time in the blood circulation ($t_{1/2\beta}$) was prolonged with respect to G-CSF. In particular, among the PEG-PLE copolymers, it can be noticed that the better results have been achieved with PLE_{10}-PEG_{20k}-Nter-G-CSF that showed a statistically significant prolonged elimination half-life with respect to PEG_{20k}-Nter-G-CSF (1.29-fold increase; $p<0.05$) and higher AUC (1.38-fold increase). Still the PEG_{40k}-Nter-G-CSF conjugates showed the best results among the studied conjugates.

Table 3. The principal pharmacokinetic parameters of G-CSF and G-CSF derivatives after i.v. administration of 100 μg/kg G-CSF (protein equiv.) in Sprague Dawley rats (n = 3 for G-CSF group; n = 4 per group for conjugates).

Compound	$t_{1/2\alpha}$ (h)	$t_{1/2\beta}$ (h)	AUC 0-inf (ng h/ml)	Cl (ml/h)	V_β (ml)
G-CSF	0.35 ± 0.04	1.91 ± 0.34	5743.5 ± 870.8	4.09 ± 0.47	11.27 ± 2.39
PEG_{40k}-Nter-G-CSF	0.54 ± 0.25	17.2 6± 1.88	43238.6 ± 7781.4	0.54 ± 0.09	13.54 ± 2.88
PEG_{20k}-Nter-G-CSF	0.34 ± 0.10	9.87 ± 0.36	23606.0 ± 5930.4	0.99 ± 0.18	14.17 ± 3.30
PLE_{10}-PEG_{20k}-Nter-G-CSF	0.28 ± 0.11	12.69 ± 1.33	32548.0 ± 2482.8	0.72 ± 0.08	13.22 ± 3.06
PLE_{20}-PEG_{20k}-Nter-G-CSF	0.14 ± 0.08	9.74 ± 0.58	26004.6 ± 6917.4	0.90 ± 0.20	12.70 ± 2.44

$t_{1/2\alpha}$ = half-life of distribution phase; $t_{1/2\beta}$ = half-life of elimination phase; AUC = area under the curve; V_β = terminal volume.

The biological activity of G-CSF consists in increasing the count of granulocytes (neutrophils, eosinophils, and basophils) and in mobilizing the progenitor cells from the bone marrow into the peripheral circulation. Indeed, the cytokine plays a critical role in differentiating myeloid cells into granulocytes, a process that is called granulopoiesis. For the pharmacodynamics evaluation of PLE-PEG block copolymers conjugates with G-CSF, hematopoietically normal mice were subcutaneously administered with 1 mg/kg (protein equiv.) of G-CSF conjugates on day 0 and the surge in the granulocyte count was observed. All the G-CSF conjugates triggered a significant increase in the myeloid cell counts in the peripheral blood. It became apparent when we analysed the count of the sub-populations of the myeloid cells that the increment depended upon higher concentrations of circulating granulocytes as the monocyte levels were unmodified. As shown in Fig. 5, on day 3 (Fig. 5A) the increment in the granulocyte count induced by the conjugates was approximately 2-fold compared to that in vehicle-receiving animals. On day 5 (Fig. 5B), the granulocyte counts returned to normal in all the groups, except for the one treated with PEG_{40k}-Nter-G-CFS which exhibited unmodified high levels

of myeloid cells and granulocytes in the blood torrent. At the end of the experiment (at day 7, Fig. 5C), the spleens were harvested, and the splenic granulocyte count was determined. In this case, the myeloid cell, granulocyte and monocyte levels were high in all the treated groups with respect to the vehicle-receiving animals. A single injection on day 0 of 1 mg/kg of G-CSF was probably not sufficient to trigger a rise in myeloid cell counts. Indeed, the effect of myeloid cells accumulation was obtained after repeated injection of 1 mg/kg of G-CSF or by increasing a lot the dose to 2.5 or 5 mg/kg for the single injection. As showed in Fig. S8, only the mice receiving a daily dose of 1 mg/kg of G-CSF experienced a marked increase in myeloid cell and circulating granulocyte levels over the 7-day period.

Overall, these data demonstrate that the activity of G-CSF derivatives synthetized with PLE-PEG block copolymers was preserved even in the presence of a negatively charged polymer and that it was comparable to that of PEG_{20k}-Nter-G-CSF as far as the stimulation of granulopoiesis was concerned.

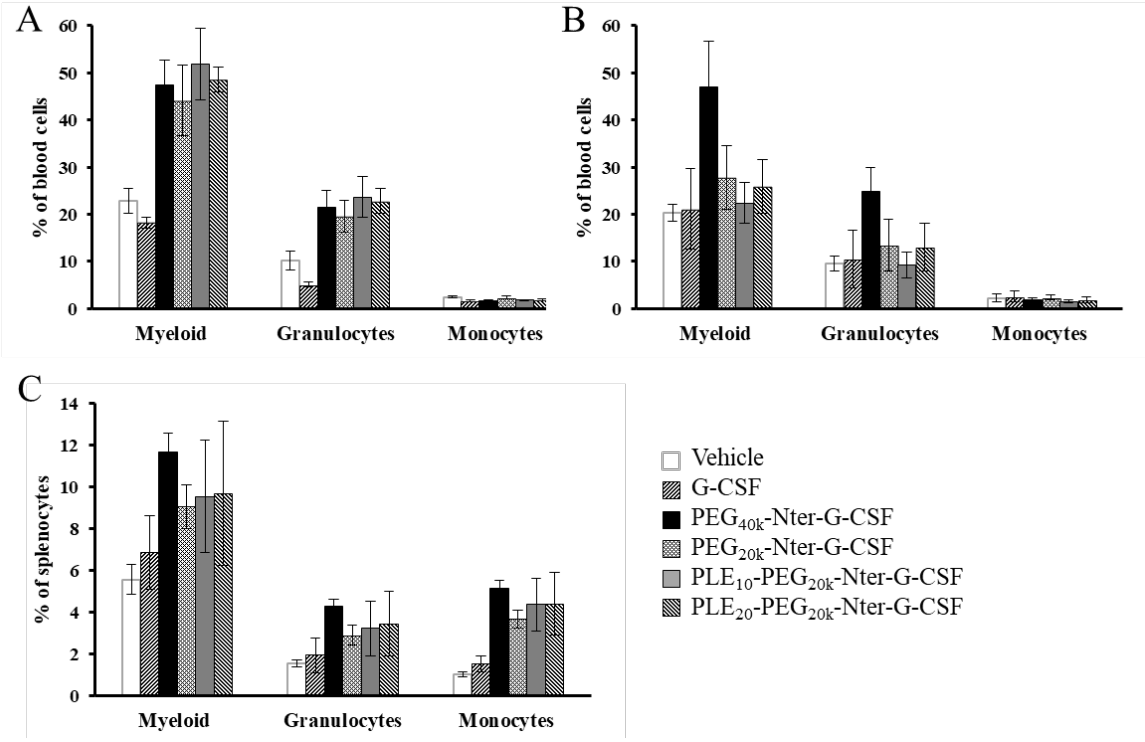

Figure 5. Levels of myeloid cells, granulocytes and monocytes in the blood on days 3 (A), 5 (B) and in the spleen on day 7 (C) in C57BL/6 mice (n = 4 per group) administered a single dose of 1 mg/kg (protein equiv.) of G-CSF, PEG_{40k}-Nter-G-CSF, PEG_{20k}-Nter-G-CSF, PLE_{10}-PEG_{20k}-Nter-G-CSF and PLE_{20}-PEG_{20k}-Nter-G-CSF. Vehicle (CTRL) was used as control.

As is known, hGH's major target organs are the bone and muscle: in fact, the protein promotes the growth of bone and muscle mass. The *in vivo* bioactivity of hGH conjugates with PLE-PEG block copolymers was investigated in hypophysectomized rats whose cumulative body weight gain and increment in tibial length were carefully assessed. A single dose of 1.8 mg/kg (protein equiv.) of polymer conjugates was injected on day 0; the unconjugated protein was administered daily for 6 days at a dose of 0.3 mg/kg. As shown in Fig. 6,

all the treatments triggered significant body weight gain in the rats with respect to the control group injected with the vehicle (PBS). Daily measurements of their body weight revealed that the groups treated with the hGH polymeric derivatives exhibited an initial rapid increase that reached a plateau at day 2, after which it remained essentially unmodified. As far as the unmodified hGH was concerned, the body weight increment was gradual over a 7-day period, reaching a plateau approximately at day 7, that is two days after the last injection. A fall in body weight was noted on days 8 and 9; the weights stabilized on days 10 and 11.

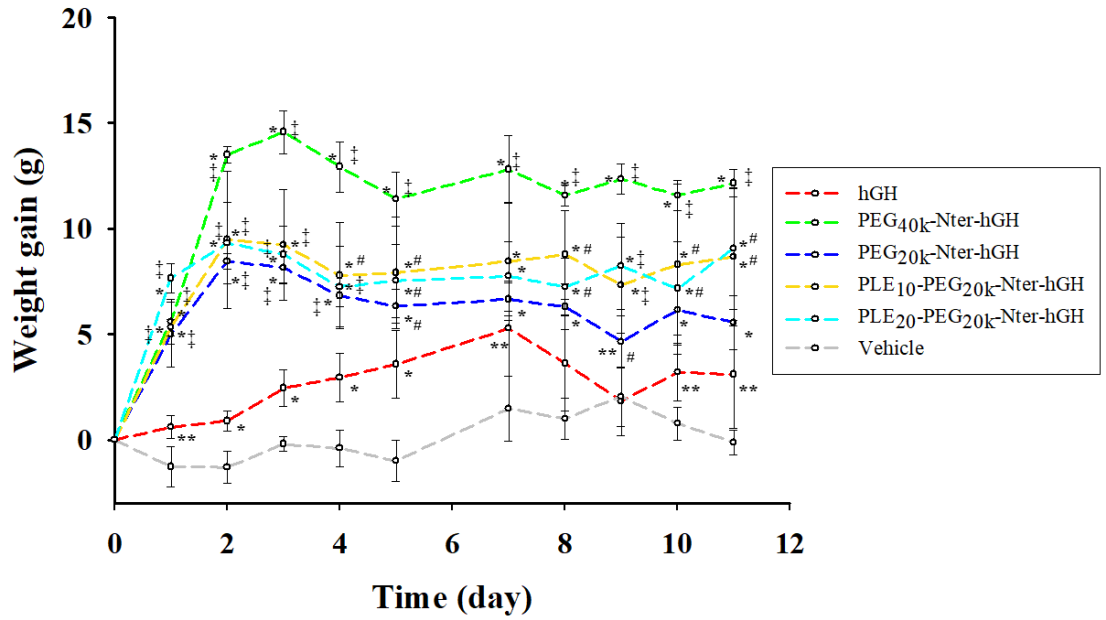

Figure 6. Average weight gain in the hypophysectomized rats (4 per group) administered six i.v. injections of 0.3 mg/kg of hGH or a single weekly dose of 1.8 mg/kg (protein equiv.) of PEG_{40k}-Nter-hGH, PEG_{20k}-Nter-hGH, PLE_{10}-PEG_{20k}-Nter-hGH and PLE_{20}-PEG_{20k}-Nter-hGH. Data are presented as mean ± SD. Symbols: * $p < 0.01$ vs. vehicle; ** $p < 0.05$ vs. vehicle; ‡ $p < 0.01$ vs. hGH; # $p < 0.05$ vs. hGH (significance was calculated using ANOVA).

The PLE-PEG block copolymer conjugates triggered a greater biological effect than did the PEG 20 kDa conjugate but a lower one with respect to PEG_{40k}-Nter-hGH. The presence of the negatively charged PLE block seemed to enhance the biological properties of the conjugate additionally with respect to PEG_{20k}-Nter-hGH.
At the end of the study (day 11) the tibias were harvested, and their lengths were measured. As shown in Fig. 7, the increments in the tibial lengths in the rodents treated with hGH and its polymeric derivatives were significant with respect to those in the PBS-treated group. Native protein promoted an increase of 1 mm and all the conjugates enhanced the effect (1 mm for PEG 20k, 1.9 mm for PEG 40kDa and 1.3 mm for both $PLE_{10}PEG_{20k}$ and $PLE_{20}PEG_{20k}$). The enhancement in tibial length in the different groups mirrored the increase in body weight, seem to confirm that $PLE_{10}PEG_{20k}$ and $PLE_{20}PEG_{20k}$ exhibited a better trend in the bioactivity compared to the neutral PEG 20 kDa conjugate, although the direct comparison is not statistically significant.

The cumulative increase in body weight and in the tibial lengths in the different groups of rodents are outlined in Table 4.

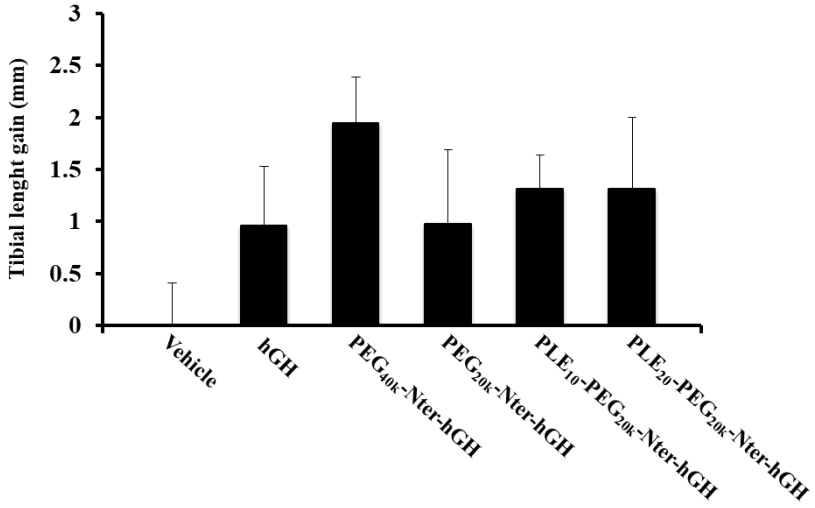

Figure 7. The increment in tibial length in the hypophysectomized rats that underwent six i.v. injections of 0.3 mg/kg of hGH or a single weekly injection of 1.8 mg/kg (protein equiv.) of PEG_{40k}-Nter-hGH, PEG_{20k}-Nter-hGH, PLE_{10}-PEG_{20k}-Nter-hGH, PLE_{20}-PEG_{20k}-Nter-hGH or PBS (n = 4 animal per group).

Table 4. The effect of six daily injections of hGH and a single injection on the first day of vehicle solution, PEG_{40k}-Nter-hGH, PEG_{20k}-Nter-hGH, PLE_{10}-PEG_{20k}-Nter-hGH and PLE_{20}-PEG_{20k}-Nter-hGH on cumulative body weight and total tibial length in hypophysectomized rats (n = 4 animal per group).

Compound	Dose and frequency	Cumulative body weight gain (g) [a)]	Tibial length (mm)
Vehicle	200 µl, day 0	-0.13 ± 0.59	38.6 ± 2.46
hGH	0.3 mg/kg × day	3.1 ± 2.53 [c)]	39.6 ± 1.23
PEG_{40k}-Nter-hGH	1.8 mg/kg, day 0	12.2 ± 0.66 [b), d)]	40.5 ± 0.68
PEG_{20k}-Nter-hGH	1.8 mg/kg, day 0	5.6 ± 1.26 [b)]	39.6 ± 1.09
PLE_{10}-PEG_{20k}-Nter-hGH	1.8 mg/kg, day 0	8.7 ± 3.27 [b), e)]	39.9 ± 2.1
PLE_{20}-PEG_{20k}-Nter-hGH	1.8 mg/kg, day 0	9.1 ± 2.86 [b), e)]	39.9 ± 0.68

[a)] Means ± Std. Dev. for four rats per group; [b)] $p<0.01$ versus vehicle; [c)] $p<0.05$ versus vehicle; [d)] $p<0.01$ versus hGH; [e)] $p<0.05$ versus hGH.

CONCLUSIONS

The current study investigated the use of negatively charged PLE-PEG block copolymers to deliver two therapeutic proteins, G-CSF and hGH. Two copolymers were used: PLE_{10}-PEG_{20k}-aldehyde, in which 10 glutamic acid monomers were attached to the PEG 20 kDa end, and PLE_{20}-PEG_{20k}-aldehyde, which presents 20 glutamic acid monomers. Our results showed that the conjugation of the multicarboxylic copolymers

produced reaction yields that were similar to those of the corresponding PEGylation reactions with neutral PEGs of similar molecular weights. Additionally, they demonstrated that the proteins' secondary structures and thermal stability were not altered by the conjugation. Finally, but no less importantly, the PLE-PEG copolymer conjugates prolonged as expected the proteins' half-lives and in particular achieved an interesting bioactive response that was comparable or superior to the one characterizing the corresponding PEG 20 kDa derivatives.

ACKNOWLEDGEMENT

The research was support in part by AIRC (IG2017, Cod. 20224), University of Padova (STARS-WiC) and NOF Corporation. The authors thank Dr. Marika Salvalaio for the care of the animal facility.

REFERENCES

[1] G. Pasut, F.M. Veronese, State of the art in PEGylation: The great versatility achieved after forty years of research, J. Control. Release. 161 (2012) 461–472. doi:10.1016/j.jconrel.2011.10.037.

[2] M.J. Harris, R.B. Chess, Effect of pegylation on pharmaceuticals, Nat. Rev. Drug Discov. 2 (2003) 214–221. doi:10.1038/nrd1033.

[3] A. Grigoletto, K. Maso, A. Mero, A. Rosato, O. Schiavon, G. Pasut, Drug and protein delivery by polymer conjugation, J. Drug Deliv. Sci. Technol. 32 (2016) 132–141. doi:10.1016/j.jddst.2015.08.006.

[4] S. Zalipsky, G. Pasut, Evolution of polymer conjugation to proteins, in: S. Zalipsky, G. Pasut (Eds.), Polym. Conjug., Elsevier, 2020: pp. 3–22. doi:10.1016/B978-0-444-64081-9.00001-2.

[5] J.K. Armstrong, G. Hempel, S. Koling, L.S. Chan, T. Fisher, H.J. Meiselman, G. Garratty, Antibody against poly(ethylene glycol) adversely affects PEG-asparaginase therapy in acute lymphoblastic leukemia patients, Cancer. 110 (2007) 103–111. doi:10.1002/cncr.22739.

[6] N. Ganson, S. Kelly, E. Scarlett, J. Sundy, M. Hershfield, Control of hyperuricemia in subjects with refractory gout, and induction of antibody against poly (ethylene glycol)(PEG), in a phase I trial of subcutaneous PEGylated urate oxidase, Arthritis Res. Ther. 8 (2005) R12.

[7] P.R. Garay, Immunogenicity of Polyethylene Glycol (PEG), Open Conf. Proc. J. 2 (2011) 104–107. doi:10.2174/2210289201102010104.

[8] P. Zhang, F. Sun, S. Liu, S. Jiang, Anti-PEG antibodies in the clinic: Current issues and beyond PEGylation, J. Control. Release. 244 (2016) 184–193. doi:10.1016/j.jconrel.2016.06.040.

[9] Q. Yang, S.K. Lai, Anti-PEG immunity: Emergence, characteristics, and unaddressed questions, Wiley Interdiscip. Rev. Nanomedicine Nanobiotechnology. 7 (2015) 655–677. doi:10.1002/wnan.1339.

[10] D.G. Rudmann, J.T. Alston, J.C. Hanson, S. Heidel, High molecular weight polyethylene glycol cellular distribution and PEG-associated cytoplasmic vacuolation is molecular weight dependent and

does not require conjugation to proteins, Toxicol. Pathol. 41 (2013) 970–983. doi:10.1177/0192623312474726.

[11] P.L. Turecek, M.J. Bossard, F. Schoetens, I.A. Ivens, PEGylation of Biopharmaceuticals: A Review of Chemistry and Nonclinical Safety Information of Approved Drugs, J. Pharm. Sci. 105 (2016) 460–475. doi:10.1016/j.xphs.2015.11.015.

[12] C. Li, Poly(L-glutamic acid)-anticancer drug conjugates, Adv. Drug Deliv. Rev. 54 (2002) 695–713. doi:10.1016/S0169-409X(02)00045-5.

[13] C. Hörtz, A. Birke, L. Kaps, S. Decker, E. Wächtersbach, K. Fischer, D. Schuppan, M. Barz, M. Schmidt, Cylindrical brush polymers with polysarcosine side chains: A novel biocompatible carrier for biomedical applications, Macromolecules. 48 (2015) 2074–2086. doi:10.1021/ma502497x.

[14] Y. Hu, Y. Hou, H. Wang, H. Lu, Polysarcosine as an Alternative to PEG for Therapeutic Protein Conjugation, Bioconjug. Chem. 29 (2018) 2232–2238. doi:10.1021/acs.bioconjchem.8b00237.

[15] A. Birke, J. Ling, M. Barz, Polysarcosine-containing copolymers: Synthesis, characterization, self-assembly, and applications, Prog. Polym. Sci. 81 (2018) 163–208. doi:10.1016/j.progpolymsci.2018.01.002.

[16] G. Tripodo, A. Trapani, M.L. Torre, G. Giammona, G. Trapani, D. Mandracchia, Hyaluronic acid and its derivatives in drug delivery and imaging: Recent advances and challenges, Eur. J. Pharm. Biopharm. 97 (2015) 400–416. doi:10.1016/j.ejpb.2015.03.032.

[17] A. Mero, M. Campisi, M. Favero, C. Barbera, C. Secchieri, J. Dayer, M. Goldring, S.R. Goldring, G. Pasut, A hyaluronic acid-salmon calcitonin conjugate for the local treatment of osteoarthritis: Chondro-protective effect in a rabbit model of early OA, J. Control. Release. 187 (2014) 30–38. doi:10.1016/j.jconrel.2014.05.008.

[18] A. Mero, M. Pasqualin, M. Campisi, D. Renier, G. Pasut, Conjugation of hyaluronan to proteins, Carbohydr. Polym. 92 (2013) 2163–2170. doi:10.1016/j.carbpol.2012.11.090.

[19] G. Gregoriadis, S. Jain, I. Papaioannou, P. Laing, Improving the therapeutic efficacy of peptides and proteins: a role for polysialic acids, Int. J. Pharm. 300 (2005) 125–130. doi:10.1016/j.ijpharm.2005.06.007.

[20] G. Gregoriadis, B. McCormack, Z. Wang, R. Lifely, Polysialic acids: potential in drug delivery, FEBS Lett. 315 (1993) 271–276. doi:10.1016/0014-5793(93)81177-2.

[21] F. Greco, I. Arif, R. Botting, C. Fante, L. Quintieri, C. Clementi, O. Schiavon, G. Pasut, Polysialic acid as a drug carrier: Evaluation of a new polysialic acid-epirubicin conjugate and its comparison against established drug carriers, Polym. Chem. 4 (2013) 1600–1609. doi:10.1039/c2py20876h.

[22] R. Luxenhofer, Y. Han, A. Schulz, J. Tong, Z. He, A. V. Kabanov, R. Jordan, Poly(2-oxazoline)s as polymer therapeutics, Macromol. Rapid Commun. 33 (2012) 1613–1631. doi:10.1002/marc.201200354.

[23] R. Hoogenboom, Poly(2-oxazoline)s: A polymer class with numerous potential applications, Angew. Chemie - Int. Ed. 48 (2009) 7978–7994. doi:10.1002/anie.200901607.

[24] A. Mero, G. Pasut, L. Dalla Via, M.W.M. Fijten, U.S. Schubert, R. Hoogenboom, F.M. Veronese, Synthesis and characterization of poly(2-ethyl 2-oxazoline)-conjugates with proteins and drugs: Suitable alternatives to PEG-conjugates?, J. Control. Release. 125 (2008) 87–95. doi:10.1016/j.jconrel.2007.10.010.

[25] A. Mero, Z. Fang, G. Pasut, F.M. Veronese, T.X. Viegas, Selective conjugation of poly(2-ethyl 2-oxazoline) to granulocyte colony stimulating factor, J. Control. Release. 159 (2012) 353–361. doi:10.1016/j.jconrel.2012.02.025.

[26] J. Pytela, R. Kotva, M. Metalová, F. Rypášček, Degradation of N5-(2-hydroxyethyl)-l-glutamine and l-glutamic acid homopolymers and copolymers by papain, Int. J. Biol. Macromol. 12 (1990) 241–251. doi:10.1016/0141-8130(90)90003-S.

[27] L.A. Mccormick-Thomson, R. Duncan, Poly(amino acid) Copolymers as a Potential Soluble Drug Delivery System. 1. Pinocytic Uptake and Lysosomal Degradation Measured In Vitro, J. Bioact. Compat. Polym. 4 (1989) 242–251. doi:10.1177/088391158900400302.

[28] B.K. Kishore, P. Lambricht, G. Laurent, P. Maldague, R. Wagner, P.M. Tulkens, Mechanism of protection afforded by polyaspartic acid against gentamicin-induced phospholipidosis. II. Comparative in vitro and in vivo studies with poly-L-aspartic, poly-L-glutamic and poly-D-glutamic acids, J. Pharmacol. Exp. Ther. 255 (1990) 875–885.

[29] S.A. Shaffer, C. Baker-Lee, J. Kennedy, M.S. Lai, P. de Vries, K. Buhler, J.W. Singer, In vitro and in vivo metabolism of paclitaxel poliglumex: identification of metabolites and active proteases, Cancer Chemother. Pharmacol. 59 (2007) 537–548. doi:10.1007/s00280-006-0296-4.

[30] J.H. Miner, The glomerular basement membrane, Exp. Cell Res. 318 (2012) 973–978. doi:10.1016/j.yexcr.2012.02.031.

[31] M. Jeansson, B. Haraldsson, Morphological and functional evidence for an important role of the endothelial cell glycocalyx in the glomerular barrier, Am. J. Physiol. - Ren. Physiol. 290 (2006) F111-116. doi:10.1152/ajprenal.00173.2005.

[32] R.L.S. Chang, W.M. Deen, C.R. Robertson, B.M. Brenner, Permselectivity of the glomerular capillary wall: III. Restricted transport of polyanions, Kidney Int. 8 (1975) 212–218. doi:10.1038/ki.1975.104.

[33] M. Ohlson, J. Sörensson, B. Haraldsson, Glomerular size and charge selectivity in the rat as revealed by FITC-Ficoll and albumin, Am. J. Physiol. - Ren. Physiol. 279 (2000) F84-91. doi:10.1152/ajprenal.2000.279.1.f84.

[34] H.G. Rennke, Y. Patel, M.A. Venkatachalam, Glomerular filtration of proteins: Clearance of anionic, neutral, and cationic horseradish peroxidase in the rat, Kidney Int. 13 (1978) 278–288. doi:10.1038/ki.1978.41.

[35] K.E. Lindström, E. Johnsson, B. Haraldsson, Glomerular charge selectivity for proteins larger than serum albumin as revealed by lactate dehydrogenase isoforms, Acta Physiol. Scand. 162 (1998) 481–488. doi:10.1046/j.1365-201X.1998.0316f.x.

[36] L.S. Nair, C.T. Laurencin, Biodegradable polymers as biomaterials, Prog. Polym. Sci. 32 (2007) 762–798. doi:10.1016/J.PROGPOLYMSCI.2007.05.017.

[37] A. Roncador, E. Oppici, M. Talelli, A.N. Pariente, M. Donini, S. Dusi, C.B. Voltattorni, M.J. Vicent, B. Cellini, Use of polymer conjugates for the intraperoxisomal delivery of engineered human alanine:glyoxylate aminotransferase as a protein therapy for primary hyperoxaluria type I, Nanomedicine Nanotechnology, Biol. Med. 13 (2017) 897–907. doi:10.1016/j.nano.2016.12.011.

[38] H.F. Gaertner, R.E. Offord, Site-specific attachment of functionalized poly(ethylene glycol) to the amino terminus of proteins, Bioconjug. Chem. 7 (1996) 38–44. doi:10.1021/bc950074d.

[39] H. Sato, Enzymatic procedure for site-specific pegylation of proteins, Adv. Drug Deliv. Rev. 54 (2002) 487–504. doi:10.1016/s0169-409x(02)00024-8.

[40] A. Grigoletto, A. Mero, H. Yoshioka, O. Schiavon, G. Pasut, Covalent immobilisation of transglutaminase: stability and applications in protein PEGylation, J. Drug Target. 25 (2017) 856–864. doi:10.1080/1061186X.2017.1363211.

[41] A. Grigoletto, A. Mero, I. Zanusso, O. Schiavon, G. Pasut, Chemical and enzymatic site specific PEGylation of hGH: the stability and in vivo activity of PEG-N-terminal-hGH and PEG-Gln141-hGH conjugates, Macromol. Biosci. 16 (2016) 50–56. doi:10.1002/mabi.201500282.

[42] P.K. Smith, R.I. Krohn, G.T. Hermanson, A.K. Mallia, F.H. Gartner, M.D. Provenzano, E.K. Fujimoto, N.M. Goeke, B.J. Olson, D.C. Klenk, Measurement of protein using bicinchoninic acid, Anal. Biochem. 150 (1985) 76–85.

[43] U.K. (1970): Laemmli, Cleavage of structural proteins during assembly of head of bacteriophage-T4, Nature. 227 (1970) 680–685. doi:10.1038/227680a0.

[44] A. Mero, B. Spolaore, F.M. Veronese, A. Fontana, Transglutaminase-mediated PEGylation of proteins: direct identification of the sites of protein modification by mass spectrometry using a novel monodisperse PEG, Bioconjug. Chem. 20 (2009) 384–389. doi:10.1021/bc800427n.

[45] A. Mero, M. Schiavon, F.M. Veronese, G. Pasut, A new method to increase selectivity of transglutaminase mediated PEGylation of salmon calcitonin and human growth hormone, J. Control. Release. 154 (2011) 27–34. doi:10.1016/j.jconrel.2011.04.024.

[46] A. Grigoletto, A. Mero, K. Maso, G. Pasut, Transgultaminase-Mediated Nanoarmoring of Enzymes by PEGylation, in: C.V. Kumar (Ed.), Methods Enzymol., Academic Press, 2017: pp. 317–346. doi:10.1016/bs.mie.2017.01.002.

[47] C.P. Hill, T.D. Osslund, D. Eisenberg, The structure of granulocyte-colony-stimulating factor and its relationship to other growth factors, Proc. Natl. Acad. Sci. U. S. A. 90 (1993) 5167–5171. doi:10.1073/pnas.90.11.5167.